24th COBEM - 2017

24th ABCM International Congress of Mechanical Engineering
December 3-8, 2017, Curitiba, PR, Brazil

COBEM-2017-0130
EXPERIMENTAL INVESTIGATION OF FORCES ACTING ON OIL DROPS WITHIN ESP IMPELLERS

Rodolfo Marcilli Perissinotto
William Monte Verde
Marcelo Souza de Castro
Antonio Carlos Bannwart
School of Mechanical Engineering, University of Campinas - UNICAMP
Rua Mendeleyev, 200 - Cidade Universitária, Campinas-SP, Brasil, CEP 13083-860
rodolfoperissinotto@gmail.com
williammonteverde@gmail.com
mcastro@fem.unicamp.br
bannwart@fem.unicamp.br

Jorge Luiz Biazussi
Center for Petroleum Studies, University of Campinas - UNICAMP
Rua Cora Coralina, 350 - Cidade Universitária, Campinas-SP, Brasil, CEP 13083-970
jorge.biazussi@gmail.com

Abstract. *This research aims to evaluate the forces that act on individual oil drops within an Electrical Submersible Pump (ESP) impeller working with a two-phase oil-water flow. An experimental study was conducted using a prototype designed to allow flow visualization within the impeller through a transparent shell. Images of drops were captured using high-speed photography and tests were performed at five rotational speeds. Images show that the oil drops become smaller when the rotation speed increases. Results for 22 oil drops reveal that the acceleration assumes magnitudes in the order of dozens or hundreds of meters per square seconds, while the resulting force has values around thousandths of Newtons. Accelerations and forces with respect to inertial and non-inertial frames of reference are quite different, because of the centrifugal and Coriolis effects. Accelerations and forces depend on the ESP rotational speed and the water flow rate and field.*

Keywords: *Electrical Submersible Pump, Two-Phase Liquid-Liquid Flow, Flow Visualization, Oil Drops.*

1. INTRODUCTION

The Electrical Submersible Pump (ESP) is a multistage centrifugal pump used for artificial lift in oil production. The ESP is an important device that provides energy to the fluids present in the reservoir, lifting them to the surface. The ESP usually works with multiphase flows, such as emulsions, which consist of mixtures of immiscible liquids. The viscosity of an emulsion with oil and water may be higher than the viscosity of the pure oil. The operation with high viscosity fluids may affect the pump behavior, causing performance losses and other problems.

Oil-in-water emulsions are composed of water with oil drops. There is an interaction between the phases. The water carries the oil drops out of the ESP impeller channels, while both phases are subjected to a pressure gradient. Pseudo-forces are present in the rotating impeller as well, when it is analyzed using a non-inertial frame of reference. The emulsion stability is a function of the fluids properties and the amount of energy dissipated in liquid-liquid flow.

The flow visualization is a relevant tool to understand the relationship between oil and water in emulsions. In this work, an experimental study is conducted with focus on flow visualization in order to investigate the motion of oil drops within an ESP impeller under different rotation speeds. Size, shape and path of oil droplets are observed, but the main objective is to evaluate accelerations and forces that govern their motion. The long-term industrial application is to find a model that estimates efficiency and performance of ESPs for use in petroleum industry. When velocities are known, the slip between phases can be estimated considering a drift-flux model.

This paper is organized into sections, which include this introduction, a brief literature review, a description of the experimental procedure, a discussion about the results and some conclusions.

2. LITERATURE REVIEW

There are many works on gas-liquid flows in the literature. Some authors studied the motion of air bubbles and the forces that govern their behavior, as Minemura and Murakami (1980), Barrios (2007), Sabino (2015), Zhang *et al.* (2016). There is a lack of available researches on liquid-liquid flows, though. In general, oil-water studies focus on drop size or breakage rate, as in Maaβ and Kraume (2012).

Minemura and Murakami (1980) investigated the dynamics of small air bubbles in a rotating impeller. According to the authors, five forces govern the motion of air bubbles in an impeller. The most important forces are the drag force due to the motion of the bubble relative to water and the pressure force due to the pressure gradient in the water surrounding the bubble. The equation of motion for water contains two terms related to the non-inertial frame of reference: the centrifugal acceleration and the Coriolis acceleration, both responsible for pseudo-forces. Additionally, the bubble motion is also influenced by a body force due to the difference in liquid densities, a force needed to accelerate the water displaced by bubble motion and, finally, a force due to a history term that shows the effect of a previous acceleration, the Basset's term.

Barrios (2007) analyzed the motion of air bubbles inside an ESP rotating impeller. The author used an ESP prototype with a transparent shell to visualize the flow within impeller channels. Images were captured with a high-speed camera. According to the author, the main forces that define the bubble trajectory are the drag and the pressure forces, acting on opposite directions.

Sabino (2015) is another example of an author who visualized the movement of air bubbles in a water flow within a rotating pump impeller. The author has identified the typical trajectories and calculated the velocity of air bubbles as a function of their position inside the impeller channel. A dependence between velocity, rotation speed and type of trajectory was observed. Sabino (2015) also agrees that two forces govern the bubble behavior: the drag force and the pressure force. The drag force is a consequence of the water velocity on the bubble and pushes it to the channel outlet. The pressure force occurs due to the pressure gradient inside the channel and pushes the air bubble back to the impeller inlet.

Zhang *et al.* (2016) investigated individual air bubbles inside a three-stage pump using a high-speed camera. The pump structure was modified to allow flow visualization through transparent parts. The researchers studied parameters as size, path and motion of air bubbles. According to them, the dominant forces acting on an isolated air bubble are the drag force, the force due to the pressure gradient and the centrifugal force. The last one is a consequence of the impeller circular motion.

Mohammadi and Sharp (2013) explored the available methods for studying the air bubble dynamics. The researchers highlighted the flow visualization with high-speed photography techniques, since they enable the observation of fast transient phenomena and offer high spatial and temporal resolutions. High-speed cameras are a powerful tool for flow visualization. Using a high-speed camera, one can identify flow patterns, track particles immersed in fluids and evaluate some variables like particle size, velocity and acceleration, for instance.

As discussed, the authors agree that drag force and pressure force are the most significant forces acting on air bubbles. The conclusion may be expanded to oil drops as well. The particle dynamics seems to define the particle characteristics, such as velocity and trajectory inside the impeller channel, which can be investigated with a flow visualization method, as a high-speed camera.

This paper aims to extend the air bubble analysis to the oil-water flow, with attention to the forces that act on oil drops.

3. EXPERIMENTAL PROCEDURE

The experiments were conducted using an ESP prototype developed by Monte Verde *et al.* (2017) in order to allow the flow visualization through a transparent shell made with organic glass. The experimental facility, shown in Fig. 1 and Fig. 2, also contains a water flow line and an oil inject system. The water circuit has water tank, booster pump and mass flow meter, while the oil circuit is composed of oil reservoir, peristaltic pump and stainless-steel capillary tubes.

Tests were carried out at University of Campinas, in Brazil, at five rotational speeds, 300 rpm, 600 rpm, 900 rpm, 1200 rpm and 1500 rpm, for water flow rates at the pump Best Efficiency Point (BEP), 1.06 m³/h, 2.13 m³/h, 3.20 m³/h, 4.26 m³/h and 5.33 m³/h. The intake manometric pressure was kept constant at 40 kPa.

The ESP rotational speed is measured with a tachometer. The water flow rate is measured with a mass flow meter and depends on the booster pump rotation speed, set through a variable speed drive. A thermocouple checks the water temperature. Two pressure transducers quantify the pressures at the ESP inlet and outlet. All the instruments include uncertainties lower than 0.5% of the measurements.

The oil is injected next to the impeller inlet at a constant flow rate of 2 ml/s, approximately. The oil has a density of 880 kg/m³ and a viscosity of 220 cP at 25 °C. The oil is darkened with a black dye to facilitate its observation in the white impeller. Flow visualization was performed using a high-speed camera IDT MotionProX® with a resolution of 1024 x 1024 pixels at the maximum acquisition rate of 1000 fps.

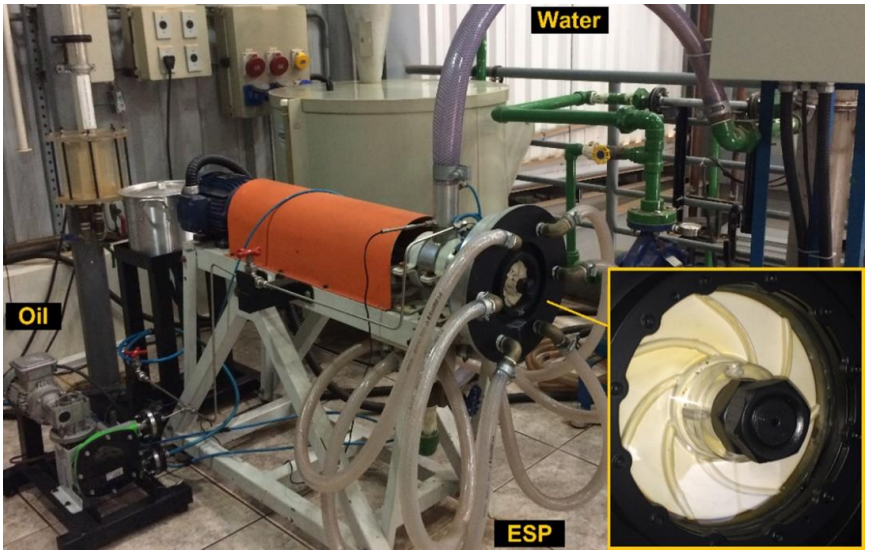

Figure 1. Photography of the experimental loop with zoom in the ESP transparent shell

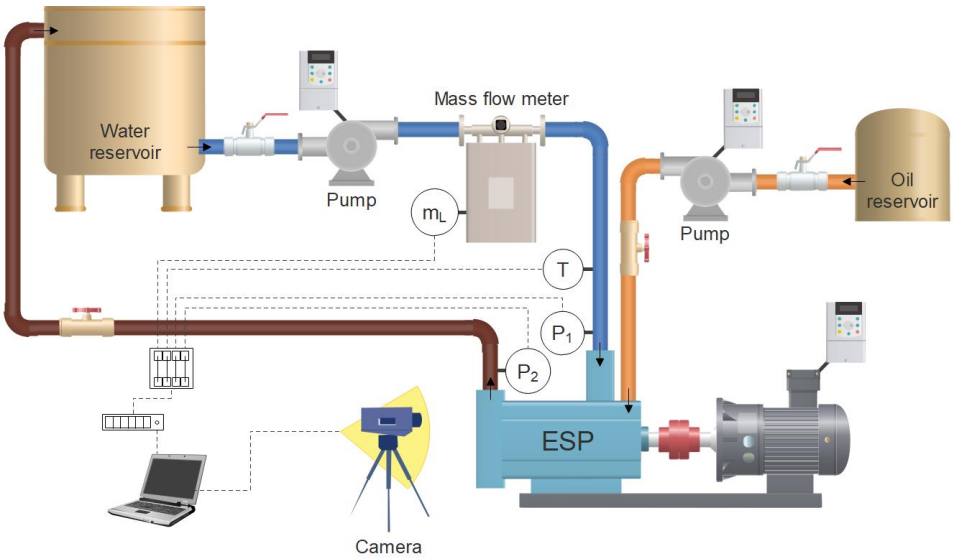

Figure 2. Schematic diagram of the experimental facility with all its components

4. RESULTS AND DISCUSSION

According to the images, the oil drops become smaller when the rotational speed increases, as can be seen in Fig. 3. Higher rotational speeds imply more intense forces acting on the oil droplets, which facilitate their breaking. The oil drops have spherical and elliptical shapes. The ESP impeller rotates clockwise.

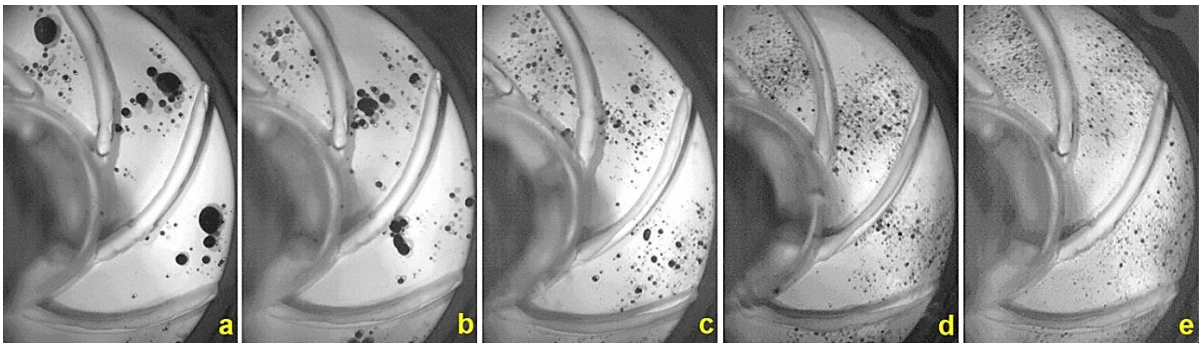

Figure 3. Impeller at (a) 300 rpm; (b) 600 rpm; (c) 900 rpm; (d) 1200 rpm; (e) 1500 rpm

Some images were processed to calculate the forces acting on drops. A LabVIEW® routine removes the rotation from the impeller and the software IDT Motion Studio® determines the oil droplet position in a Lagrangian approach, by identifying differences between consecutive images. The position, R and θ, is quantified in a polar non-inertial coordinate system, as presented by Fig. 4. Thus, the position values are used to obtain the velocity, V, and the acceleration, A, given by Eq. (1) and Eq. (2).

$$\mathrm{V} = V_R\,\hat{\imath}_\mathrm{R} + V_\theta\,\hat{\imath}_\theta = \dot{R}\,\hat{\imath}_\mathrm{R} + R\dot{\theta}\,\hat{\imath}_\theta \tag{1}$$

$$\mathrm{A} = A_R\,\hat{\imath}_\mathrm{R} + A_\theta\,\hat{\imath}_\theta = \left(\ddot{R} - R\dot{\theta}^2\right)\hat{\imath}_\mathrm{R} + \left(R\ddot{\theta} + 2\dot{R}\dot{\theta}\right)\hat{\imath}_\theta \tag{2}$$

Then, the acceleration measured in the non-inertial rotating system, A, is converted to a new acceleration related to a fixed inertial coordinate system, A_I, as introduced in Eq. (3), which includes a centrifugal effect, ω×(ω×R), and a Coriolis effect, 2ω×V. The dots indicate time derivatives, calculated numerically using finite-difference methods.

$$\mathrm{A_I} = \left[\ddot{R} - \left(\omega + \dot{\theta}\right)^2 R\right]\,\hat{\imath}_\mathrm{R} + \left[R\ddot{\theta} + 2\left(\omega + \dot{\theta}\right)\dot{R}\right]\hat{\imath}_\theta \tag{3}$$

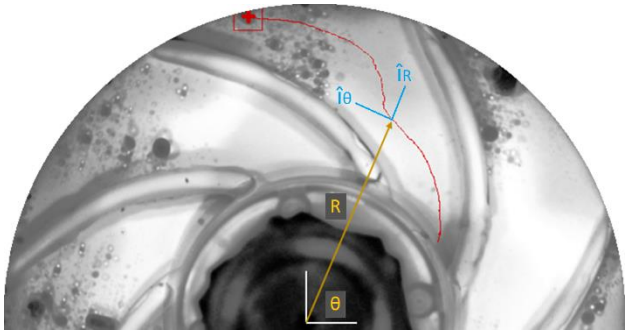

Figure 4. Position of an oil drop in a polar coordinate system

The acceleration is a consequence of the forces acting on the oil drops. Therefore, once the acceleration is known, the forces can be estimated too. The resultant force, F_R, is a function of the oil density, ρ_o, and the drop diameter, d, according to Eq. (4), the Newton's second law.

$$\mathrm{F_R} = \rho_\mathrm{o}\left(\frac{\pi \mathrm{d}^3}{6}\right)\mathrm{A_I} \tag{4}$$

4.1 Results for 600 rpm

The next paragraphs discuss the results for a sample of 12 oil droplets. The particles were tracked at 600 rpm and 2.13 m³/h. At those conditions, the drops have diameters from 1 mm to 3 mm approximately. The chosen oil drops perform a central path, as displayed in Fig. 5.

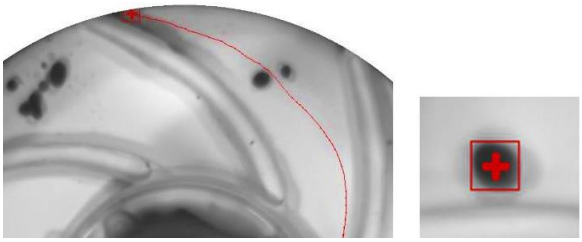

Figure 5. Tracking of an oil droplet with a central trajectory

The inertial acceleration takes values around dozens of meters per second squared, as Fig. 6 exhibits. The radial and the transverse accelerations present negative quantities in almost the entire impeller radius. Second order polynomials reveal the average behavior.

The centrifugal and the Coriolis effects have a significant influence on the inertial acceleration, A_I. The centrifugal acceleration acts radially. Its magnitude increases with the impeller radius. The Coriolis acceleration has two components. The radial component is a function of the oil drop transverse velocity, while the transverse component depends on the oil drop radial velocity.

Both radial and transverse velocities have magnitudes around one meter per second, when they are measured in the non-inertial rotating frame of reference. Thus, the centrifugal effect reaches a maximum value of 220 m/s² at the channel outlet, while the Coriolis components attain numerical quantities about 150 m/s², as Fig. 6 shows as well.

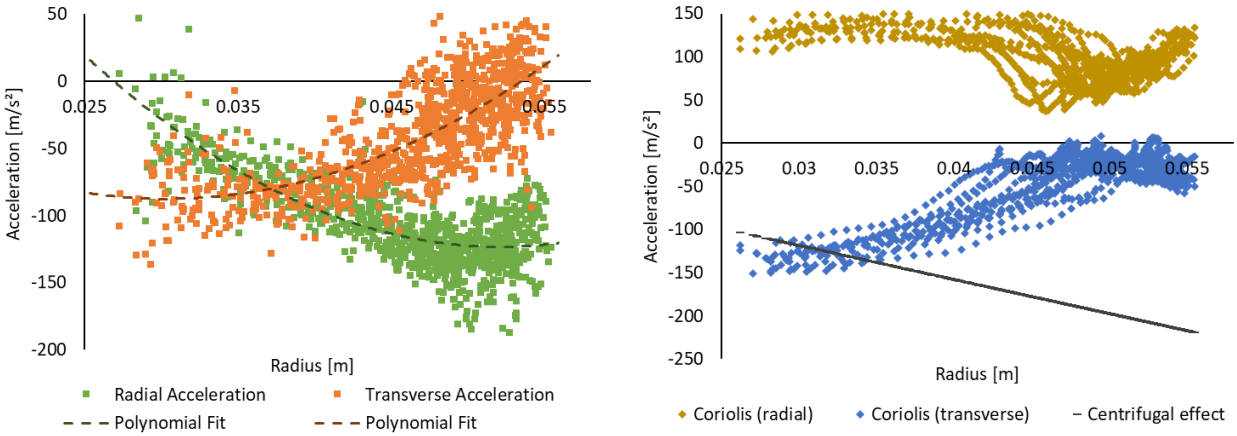

(a) (b)

Figure 6. Inertial accelerations of oil drops at 600 rpm (a), centrifugal and Coriolis effects added to A to obtain A_I (b)

Finally, Fig. 7 exposes the resultant force that acts on the oil drops. The force depends on the oil droplet mass, which is a function of the diameter. The smallest drop, with a diameter of 1 millimeter, has a mass around 0.46 microgram and the force that governs its movement gets values from 3.10^{-5} to 8.10^{-5} Newton. On the other hand, the biggest drop, with 3 mm, has a mass of 12 micrograms and the force assumes a magnitude from 1.10^{-3} to 3.10^{-3} N.

As can be seen, although the force is very low, it is sufficient to cause a high acceleration.

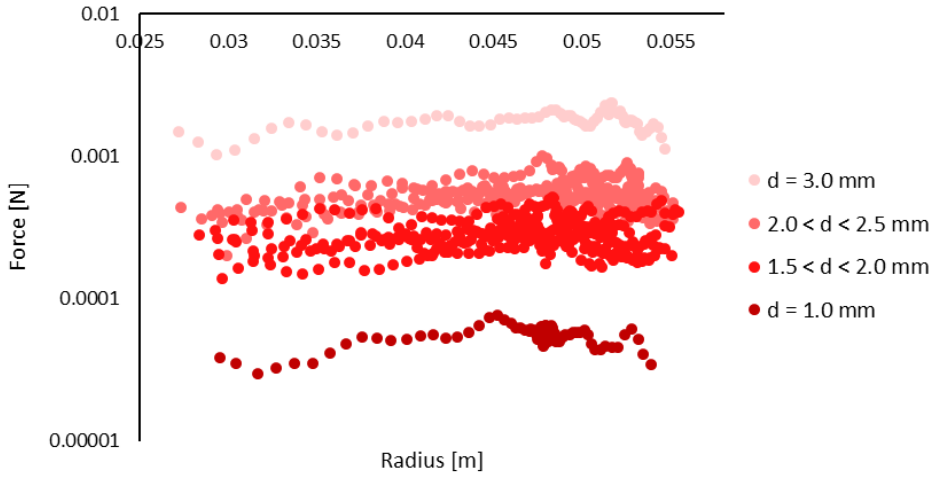

Figure 7. Resultant forces of oil drops at 600 rpm

4.2 Results for 1200 rpm

The procedure was repeated to a sample of 10 oil droplets at 1200 rpm and 4.26 m³/h. The selected oil drops present a central path and have diameters from 1 mm to 2 mm. At 1200 rpm, the inertial acceleration gets values in the order of hundreds of meters per second squared. In other words, approximately four times larger than the numbers found before, in the 600-rpm case.

In the 1200-rpm case, the radial and transverse velocities have magnitudes around two meters per second, twice the velocities calculated at 600 rpm. At 1200 rpm, the centrifugal effect and the Coriolis components reach the highest quantities of 880 m/s² and 680 m/s², respectively. Below, Fig. 8 displays the results.

Lastly, Fig. 9 exhibits the resultant force that governs the oil drops movement at 1200 rpm. The smallest drop, with a diameter of 1 mm, is controlled by a force with magnitude from 3.10^{-4} to 4.10^{-4} Newton. Meanwhile, the biggest drop, with 2 millimeters, is influenced by a force with 2.10^{-3} to 3.10^{-3} N approximately. It can be noticed that the forces are much larger in the 1200-rpm case.

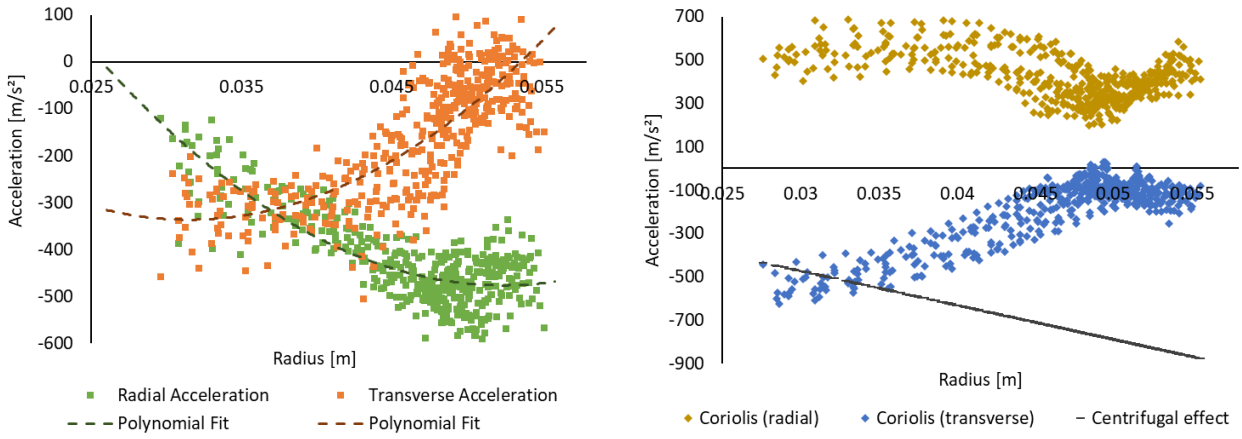

(a) (b)

Figure 8. Inertial accelerations of oil drops at 1200 rpm (a), centrifugal and Coriolis effects added to A to obtain A_I (b)

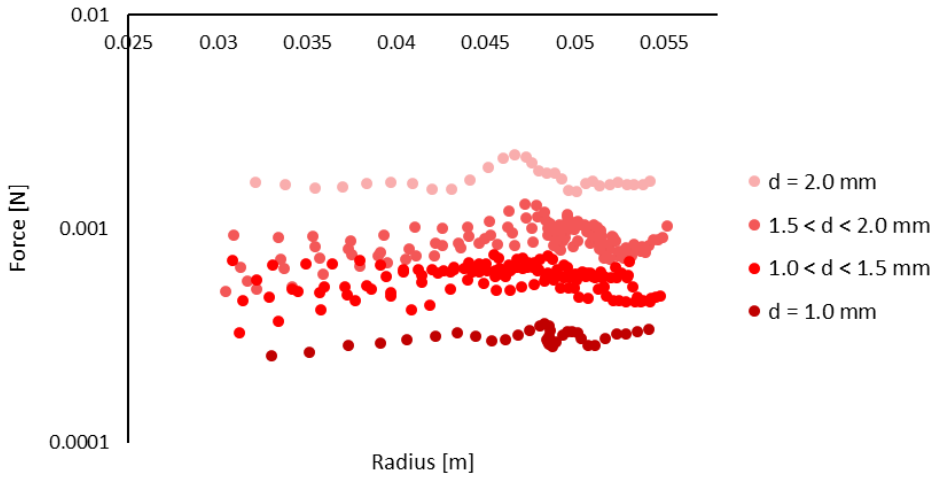

Figure 9. Resultant forces of oil drops at 1200 rpm

It is observed that the oil droplet velocities, accelerations and forces are proportional to the ESP rotational speed and to the water flow rate. An increase in velocities causes twice as much increase in accelerations. The resultant forces are affected by acceleration increments as well. The centrifugal and Coriolis phenomena are also notable for their magnitude, especially at high impeller rotation speeds.

As discussed before, the inertial acceleration assumes negative quantities. Therefore, it acts radially to the impeller center and transversally to clockwise direction. The resulting force has the same directions, but also depends on the oil droplet mass, function of its volume and density. The resultant force is a sum of several forces, but the most important are the drag force and the pressure force, according to Minemura and Murakami (1980), Barrios (2007), Sabino (2015) and Zhang *et al.* (2016), cited in the Literature Review.

5. CONCLUSIONS

The images revealed that the oil droplets become smaller when the rotation speed increases. Each drop has velocities, accelerations and forces that can be evaluated through the comparison between two consecutive images. For the tracked oil drops, the velocities, accelerations and forces are proportional to the ESP rotational speed and the water flow rate.

Results for 22 oil drops reveal that the accelerations get quantities around dozens or hundreds of meters per second squared, while the resultant forces have values in the order of thousandths of Newton. The inertial and the non-inertial accelerations are significantly different, because of the centrifugal and the Coriolis effects, with high magnitudes.

The inertial acceleration acts radially to the impeller center and transversally to clockwise direction. The resulting force has the same directions, but is also a function of the oil drop mass, which depends on its volume and density. The resultant force is a sum of the drag force and the pressure force, among other less important forces.

6. ACKNOWLEDGEMENTS

The authors thank Statoil Brazil, ANP ("Compromisso de Investimentos com Pesquisa e Desenvolvimento") and PRH/ANP for providing financial support for this work. Acknowledgments are also extended to CEPETRO/UNICAMP and ALFA - Artificial Lift & Flow Assurance Research Group.

7. REFERENCES

Barrios, L.J., 2007. “Visualization and modeling of multiphase performance inside an electrical submersible pump”. PhD Thesis. University of Tulsa.

Maaß, S., Kraume, M., 2012. “Determination of breakage rates using single drop experiments”. Chemical Engineering Science, Vol. 70, pp. 146-164.

Minemura, K., Murakami, M., 1980. “A theoretical study on air bubble motion in a centrifugal pump impeller”. ASME Journal of Fluids Engineering, Vol. 102, pp. 446-455.

Mohammadi, M., Sharp, K.V., 2013. “Experimental techniques for bubble dynamics analysis in microchannels: a review”. Journal of Fluids Engineering, 135/021202-1.

Monte Verde, W., Biazussi, J.L., Sassim, N.A., Bannwart, A.C., 2017. “Experimental study of gas-liquid two-phase flow patterns within centrifugal pumps impellers”. Experimental Thermal and Fluid Science, Vol. 85, pp. 37-51.

Sabino, R.H.G., 2015. “Análise da dinâmica de uma bolha de gás em uma bomba centrífuga”. Master’s thesis. Universidade Tecnológica Federal do Paraná.

Zhang, J., Cai, S., Li, Y., Zhu, H., Zhang, Y., 2016. “Visualization study of gas-liquid two-phase flow patterns inside a three-stage rotodynamic multiphase pump”. Experimental Thermal and Fluid Science, Vol. 70, pp. 125-138.

8. RESPONSIBILITY NOTICE

The authors are the only responsible for the printed material included in this paper.